Vibrational spectroscopy of excited electronic states in carotenoids in vivo

Picosecond time-resolved resonance Raman scattering

H. Hayashi,*‡ T. Noguchi,* M. Tasumi,‡ and G. H. Atkinson*

*Department of Chemistry and Optical Science Center, University of Arizona, Tucson, Arizona 85721 USA; ‡Department of Chemistry, The University of Tokyo, Bunkyo-ku, Tokyo 113, Japan; #Lady Davis Professor, Hebrew University and Technion, Israel, 1990; +Senior Fulbright Professor, Federal Republic of Germany, 1990

ABSTRACT The vibrational spectroscopy and population dynamics of excited singlet (2^1A_g), excited triplet (^3B_u), and the ground (^1A_g) electronic states of carotenoids in chromatophores of *Chromatium vinosum* (mainly spirilloxanthin and rhodopin) and of the same carotenoids in benzene solutions are examined by picosecond time-resolved resonance Raman scattering. Coherent Stokes Raman scattering from the ground states of carotenoids in chromatophores also is observed. Resonance Raman spectra of in vitro rhodopin and spirilloxanthin when compared with in vivo data demonstrate that scattering from spirilloxanthin dominates the in vivo spectrum. Comparisons of the time-dependent intensities of 2^1A_g and ^1A_g resonance Raman bands from both in vitro and in vivo carotenoids suggest that vibrationally excited levels in ^1A_g are populated directly by the decay of the 2^1A_g state and that these levels relax into a thermalized distribution in <50 ps. The appearance of asymmetrically broadened, ground-state resonance Raman bands supports this conclusion. Formation of the ^3B_u state is observed for carotenoids in chromatophores, but not for in vitro spirilloxanthin indicating that the ^3B_u state is formed by fission processes originating from the spatial organization of pigments within chromatophores. The rate at which the intensities of 2^1A_g resonance Raman bands decay is faster for the carotenoids in vivo than for those in vitro thereby indicating that additional relaxation channels (e.g., energy transfer to bacteriochlorophylls) are present in the chromatophore. The similarity of the in vivo and in vitro 2^1A_g resonance Raman spectra shows that no significant modifications in the vibronic coupling has been caused by the chromatophore environment.

INTRODUCTION

The molecular mechanism(s) underlying the biochemical function of carotenoids in the antenna pigment-protein complexes of photosynthetic bacteria involves the transient population of at least three excited electronic states (1, 2). These excited-state carotenoids are involved in photosynthetic systems in two major ways: (*a*) light-harvesting in which radiative energy is absorbed via the allowed $^1B_u \leftarrow {}^1A_g$ transition and subsequently transferred through the 2^1A_g excited state to bacteriochlorophylls (Bchls) and (*b*) protection from photodamage through the formation of excited ^3B_u states (1, 2). The energetic positions and population dynamics of these excited electronic states are, therefore, of importance to an understanding of the biochemical functionality of carotenoids.

The 2^1A_g state has been subjected to an especially large number of studies involving absorption (3–12) and resonance Raman (RR) (13–24) because it is widely thought to be directly involved in the singlet energy transfer process (25–27). Because the electronic transition between 2^1A_g and ^1A_g is symmetry forbidden, the 2^1A_g state is populated by the rapid (<300 fs [26]) photophysical relaxation of the ^1B_u state which can be optically populated via the allowed transition from the ground (^1A_g) state ($\lambda = 400$–500 nm). Transient absorption measurements have shown that the 2^1A_g state in β-carotene has a lifetime of ≈ 10 ps in organic solvents (4, 7, 8). The in vivo lifetimes of 2^1A_g carotenoids have been reported to be 3–7 ps in pigment-protein complexes of *Rhodopseudomonas acidophila* (5, 6), 0.2–0.3 ps in complexes of *Rhodobactor sphaeroides* (10), and 0.2–2.0 ps in thylakoid membranes from *Phaeodactylum tricornutum* and *Nannochloropsis sp.* (11). The 2^1A_g lifetime is thought to shorten in chromatophores due to enerегy transfer processes. The relative energy of the 2^1A_g state has been derived from the RR excitation profiles of β-carotene (13). The 2^1A_g state is placed 3,470 cm^{-1} lower in energy than the $^1B_u^+$ state (13).

Recently, the vibrational spectroscopy of the 2^1A_g state has been examined by picosecond time-resolved resonance Raman (PTR^3) scattering (17–24). The C = C stretching frequencies in the 2^1A_g states of a variety of carotenoids have been shown by PTR^3 spectroscopy to correlate well with those of shorter polyenes examined by low-temperature fluorescence spectroscopy (24). In addition, the C = C stretching frequencies for all of these carotenoids are well described by a vibronic coupling model which considers interactions between

Address correspondence to Dr. M. Tasumi and Dr. G. H. Atkinson. Dr. Atkinson is a Lady Davis Professor at Hebrew University and Technion, Israel, 1990.
Dr. Atkinson is a Senior Fulbright Professor, Federal Republic of Germany, 1990.

0006-3495/91/07/252/09 $2.00

the ^1A_g, ^1B_u, and 2^1A_g states including the influence of solvent polarizability (23). For example, the substantially larger C = C stretching frequencies observed in the 2^1A_g states (relative to the ^1A_g) can be attributed to strong vibronic coupling between ^1A_g and 2^1A_g whereas the solvent effect on this C = C frequency is well described by the vibronic coupling between ^1B_u and 2^1A_g (23).

The quantum yield for ^3B_u formation by intersystem crossing in isolated carotenoids is extremely low (< 0.001 [28]). In chromatophores, however, there are two pathways by which the ^3B_u state can be populated: (*a*) energy transfer from triplet Bchl (2) and (*b*) singlet fission of a 2^1A_g carotenoid state to form a triplet pair with another carotenoid (i.e., homofission) or a Bchl molecule (i.e., heterofission) (3, 9, 29–32). Whereas the former is a necessary process in the photodamage protection mechanism of membranes, the biological significance of the latter remains unclear. Both processes require the spatial organization of the carotenoids and chlorophylls found within the light-harvesting proteins.

Previous studies, therefore, provide some characterization of the excited electronic states, but much remains unknown, especially in the in vivo systems. Of particular value is the time-resolved, spectroscopic identification of specific excited states (electronic and vibrational) and the direct correlation between their time-dependent populations. In this paper, PTR[3] spectroscopy is used to measure the vibrational structure and population dynamics of the 2^1A_g and ^3B_u excited states and of the ^1A_g ground state (including vibrationally excited levels) of the carotenoids (spirilloxanthin and rhodopin) in chromatophores of *Ch. vinosum* and of the same carotenoids isolated in benzene solutions (in vitro).

EXPERIMENTAL

The intracytoplasmic membranes (chromatophores) are prepared from *Ch. vinosum* as reported previously (33) and suspended in a 50 mM *tris* buffer (pH 8.4) to give a sample absorbance of 10 at 590 nm with a 10 mm light path. Spirilloxanthin and rhodopin are extracted from *Ch. vinosum* and purified as described previously (27). These carotenoids are dissolved in benzene to give the absorbance of 20 at their absorption maxima with a 10 mm light path. A flowing liquid jet is formed for PTR[3] measurements by circulating the suspension through a 300 ± 50 μm (ID) glass nozzle. The sample reservoir and pump head are immersed in ice water to maintain the sample at a constant temperature of 12°C. The velocity of the sample jet is fast enough ($\approx$20 m/s) to prevent two successive pairs of laser pulses from illuminating the same volume when the pump and probe laser systems are both operated at 1 MHz repetition rates.

The instrumentation is described in detail elsewhere (34, 35). Briefly, two dye lasers (model 703-3; Coherent Inc., Palo Alto, CA) are synchronously pumped by the second harmonic frequency of the mode-locked, Nd:YAG laser (Quantronix model 416 and SHG model 324) to produce 6 ps (FWHM) pulses at 1 MHz repetition rates from each. One dye laser (565 nm, 5–10 mW) is used as a pump for the excitation of carotenoids and the other (595–620 nm, 2–4 mW) is used as a probe laser to generate RR scattering. The pump and probe laser beams are aligned collinearly before being focused into the liquid jet with a microscope objective. The beam waists of the focused laser beams within the sample jet volume are $\approx$20 μm. The picosecond delay times between the pump and probe laser pulses are obtained with an optical delay line.

The RR scattering is collected at 90° to the plane formed by the sample jet and the two laser beams. A triple monochromator (Spex Triplemate) is used to disperse the RR scattering before detection by an intensified reticon array (model 1463; EG&G Electro-Optics, Salem, MA). The reticon signal is processed by an optical multichannel analyzer before being transferred to a computer for data storage and analysis. Contributions from the pump laser are subtracted from the total RR scattering measured at a given time delay in order to obtain the RR spectrum generated by the probe laser excitation alone.

Each spectrum reported here is an average of four to five sets of data each one of which requires 400 s to record. The total data acquisition time for one spectrum, therefore, is $\approx$30 min.

RESULTS AND DISCUSSION

A. Assignment of RR spectra

RR scattering from chromatophores of *Ch. vinosum* is recorded under several different single and two (pump/probe) laser conditions. These experiments are designed to optimize the measurement and to facilitate the characterization of RR scattering from excited electronic state carotenoid populations in these chromatophores.

Single, pulsed (6 ps FWHM) laser excitation at 565 nm (1 MHz repetition rate) is used at two different power levels (2 and 10 mW) to record the RR spectra presented in Fig. 1. The intensities of the resultant RR features do not scale quantitatively with the excitation power (i.e., the 10 mW features are only 4.3 times larger than the corresponding 2 mW features). This discrepancy can be attributed to the optical depletion of the

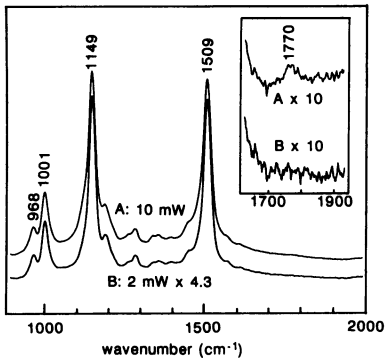

FIGURE 1 Resonance Raman (RR) spectra of carotenoids in chromatophores from *Ch. vinosum* measured using a single, pulsed laser excitation at 565 nm (6 ps pulsewidth, 1 MHz repetition rate). Chromatophores are suspended in a *tris* buffer (pH = 8.4) and have an absorbance of ≈ 10 at 590 nm. The sample suspension is circulated by a mechanical pump through a glass nozzle to form a jet (≈300 μm diam) while its temperature is held constant at ≈12°C. (*A*) RR spectrum measured with 10 mW laser power. (*B*) RR spectrum measured with 2 mW laser power and multiplied by a factor of 4.3 in order to scale the major RR bands to approximately the same intensities.

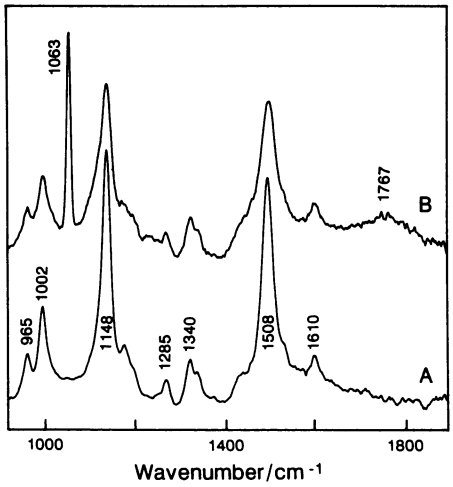

FIGURE 2 Resonance Raman (RR) and picosecond time-resolved resonance Raman (PTR^3) spectra of chromatophores from *Ch. vinosum*. Sample conditions are the same as those described in Fig. 1. (*A*) RR spectrum measured with only a 601 nm probe laser (6 ps FWHM, 3.5 mW, 1 MHz repetition rate). (*B*) PTR^3 spectrum measured with a 0 ps delay between each 601 nm probe laser pulse (6 ps FWHM, 3.5 mW) and a 565 nm pump pulse (6 ps FWHM, 7 mW, 1 MHz repetition rate). Emission generated by the 565 nm pump pulse is measured separately and subtracted from the PTR^3 signal to obtain the spectrum presented.

ground-state population and the corresponding transient population of excited state(s) within the 6 ps duration of the 565 nm excitation.

Although most of the RR bands in both spectra can be assigned to ground-state vibrational modes of the membrane carotenoids, at least one new feature appears near 1,770 cm^{-1} in the 10 mW spectrum (Fig. 1, ×10 expanded insert). This 1,770 cm^{-1} band can be assigned to the C = C stretching mode in the excited 2^1A_g carotenoid state based on the appearance of analogous transient RR bands from the 2^1A_g states of isolated, in vitro carotenoids (e.g., at 1,777 cm^{-1} for β-carotene in benzene solution (17, 18); also see Table 1 in reference [24]).

RR scattering from the excited electronic states of in vivo membrane carotenoids can be observed in more detail using picosecond pump/probe experiments (i.e., PTR^3). To enhance RR scattering from the 2^1A_g state, a 601 nm probe wavelength (resonant with $S_n \leftarrow 2^1A_g$) is selected for use with 565 nm pumping (resonant with $^1B_u \leftarrow {}^1A_g$). The RR spectrum recorded with 3.5 mW of 601 nm probe laser alone (Fig. 2*A*) is almost the same as that obtained with 2 mW of 565 nm excitation (Fig. 1). The relatively stronger 1,340 and 1,610 cm^{-1} RR bands in the single laser 601 nm spectrum are exceptions which can be attributed to RR scattering from the BChls. The spectral resonance between the 601 nm excitation and the Q_x transition of BChl near 590 nm is better than for the 565 nm excitation.

The PTR^3 spectrum (565 nm pump/601 nm probe) obtained at 0 ps time delay (Fig. 2*B*) contains two features which are significantly different than those found in either the 565 or 601 nm low power, single laser results (Fig. 1*B* and 2*A*): (*a*) an intense feature at 1,063 cm^{-1} with a narrow bandwidth and (*b*) a feature at 1,767 cm^{-1} with broad bandwidth.

The intensity of the 1,063 cm^{-1} band is comparable to the spontaneous RR bands and its frequency displacement corresponds to the energetic difference between the pump and probe laser wavelengths. With other combinations of pump and probe laser wavelengths, similar bands appear at the corresponding energy differences (frequency displacements). Three examples are shown in Fig. 3. Specifically, when the difference between the pump/probe laser wavelengths match the Raman frequency displacement assigned to the C–C stretching mode of ^1A_g carotenoids at 1,148 cm^{-1}, a sharp band > 10 times stronger than the corresponding spontaneous RR band appears (Fig. 3*B*). These narrow bandwidth features are present only during the cross-correlation time (≈ 8 ps) of the pump/probe laser pulses (*vide infra*) and are not found for single laser excitation even at high power excitation (Fig. 1). Based on these observations, the 968, 1,063, 1,148, and 1,400 cm^{-1} bands in Figs. 2 and 3 are all attributable to coherent Stokes Raman scattering (CSRS) and do not arise from spontaneous RR scattering observed elsewhere in these spec-

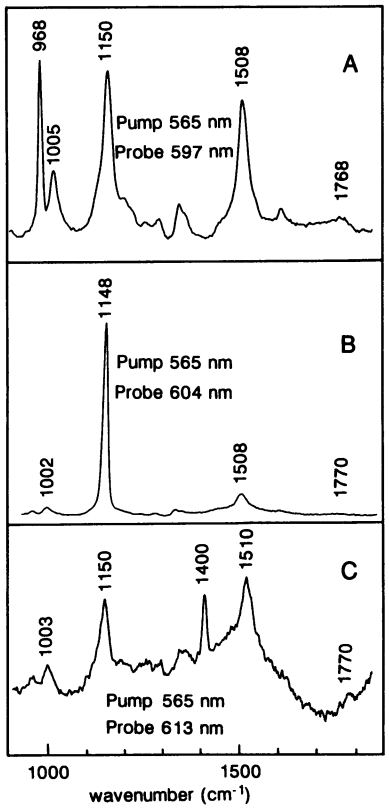

FIGURE 3 Picosecond time-resolved resonance Raman (PTR^3) spectra of carotenoids in chromatophores from *Ch. vinosum* measured with a 0 ps delay between the 565 nm pumping pulse (6 ps FWHM) and the probe laser pulse operating at a variety of wavelengths: (*A*) 597 nm, (*B*) 604 nm, and (*C*) 613 nm. The frequency differences between the pump and probe laser wavelengths are: (*A*) 965 cm^{-1}, (*B*) 1,150 cm^{-1}, and (*C*) 1,400 cm^{-1}. Sample conditions and laser parameters are described in Figs. 1 and 2, respectively.

tra. It should be noted that only a small percentage of the CSRS signal is recorded because this signal is observed at 90° to the exciting laser beams. In addition, the phase matching condition required for CSRS is fulfilled only for the chromatophoric solutions which are slightly turbid. This point is discussed again (*vide infra*).

By contrast, the relatively small band at $\approx$1,770 cm^{-1} is present for all combinations of pump and probe laser wavelengths used and thereby, cannot be assigned to coherent Raman scattering, but rather is a resonantly enhanced spontaneous Raman signal. This band also is observed in the high power, single laser spectrum (Fig. 1) and is assigned to the 2^1A_g states of the two major carotenoids found in *Ch. vinosum,* namely spirilloxanthin and rhodopin.

A more specific assignment, in terms of which of the two carotenoids contribute the most to the RR spectrum, can be obtained from the PTR^3 spectra of spirilloxanthin and rhodopin in benzene solution. These spectra are recorded at 0 ps time delay with the same combination of laser wavelengths (565 nm pump and 601 nm probe) as in the in vivo measurements. The benzene solutions examined also have the same absorbance at their maxima as the in vivo sample. The PTR^3 data are presented in Fig. 4.

Clearly, the overall intensities of the RR features from spirilloxanthin are much larger than those from rhodopin both in the ground state and in the excited 2^1A_g state. These results are reasonable because the ground- and excited-state absorbances of spirilloxanthin are in better resonance, respectively, with the 565 nm pump and 601 nm probe laser wavelengths than those of rhodopin. RR scattering from the 2^1A_g state of rhodopin alone can be observed more clearly when pump and probe laser wavelengths (i.e., 425 nm pump and 572 nm probe) are selected which directly correlate with the rhodopin absorptions (24). Thus, even though the *Ch. vinosum* chromatophore contains the two carotenoids in roughly equal amounts (spirilloxanthin:rhodopin $\approx$ 2:3), the RR features from both the ^1A_g and 2^1A_g states observed in Figs. 2 and 3 arise primarily from spirilloxanthin.

B. Population dynamics from PTR^3 spectra

PTR^3 data from the in vivo chromatophore, recorded with time delays ranging from −14 ps (i.e., probe laser

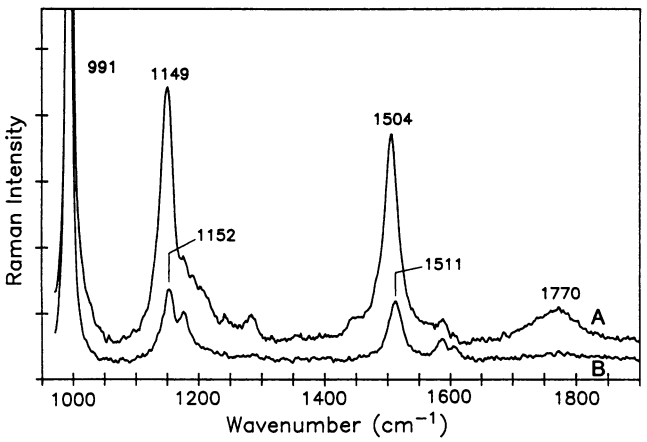

FIGURE 4 Picosecond time-resolved resonance Raman (PTR^3) spectra of carotenoids extracted from *Ch. vinosum* in a benzene solvent. (*A*) PTR^3 spectrum of spirilloxanthin. (*B*) PTR^3 spectrum of rhodopin. Both spectra are measured with a 0 ps delay between the 601 nm probe pulses and the 565 nm pump pulses. The benzene samples of both spirilloxanthin and rhodopin have absorbances of $\approx$20 at their absorption maxima (510 and 485 nm, respectively). The strong band at 991 cm^{-1} is due to the benzene solvent. Sample conditions and laser parameters are described in Figs. 1 and 2, respectively.

pulse arrives at the sample 14 ps before the pump laser pulse) to 50 ps are presented in Fig. 5. These data appear in Fig. 5 as difference PTR[3] spectra obtained by subtracting the RR spectrum recorded with low-energy, probe laser only excitation (scaling factor of one) from the PTR[3] spectrum recorded at each time delay. The negative intensities of the ground-state carotenoid RR bands at 1,508, 1,148, 1,002 and 965 cm^{-1} in the 0 ps delay spectrum, therefore, reflect the depletion of the ground-state ^1A_g population by 565 nm optical pumping. By contrast, positive bands (e.g., 1,767, 1,468, 1,245, and 1,119 cm^{-1}) arise from transient species or populations which exist during the cross-correlation period ($\approx$8 ps) defined by the pump and probe laser pulses. Bands with positive intensities also can appear as a result of coherent Raman scattering involving a ground-state vibrational mode (e.g., 1,063 cm^{-1} is CSRS).

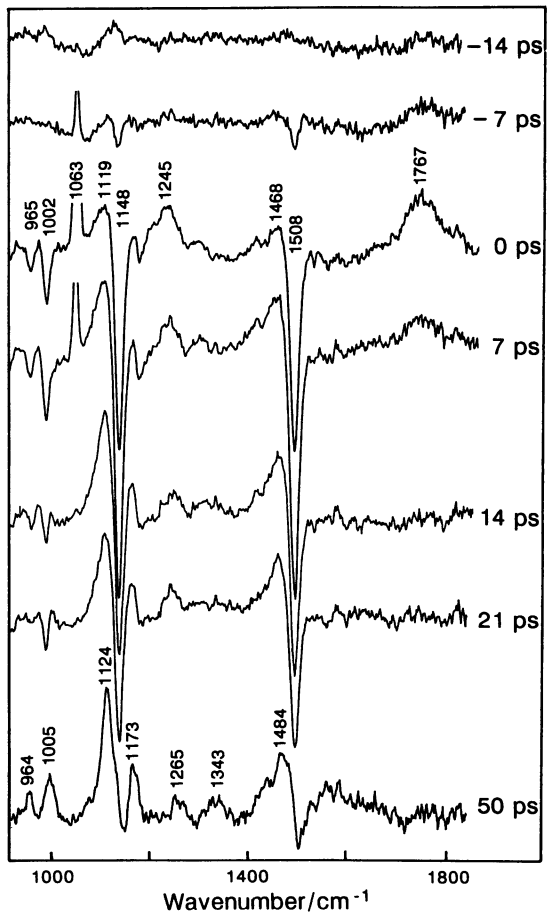

FIGURE 5 Population dynamics of excited and ground-states of carotenoids in chromatophores from *Ch. vinosum* as viewed in PTR[3] spectra. The data are presented as difference spectra obtained by subtraction of the probe only spectrum measured at 601 nm from the PTR[3] spectrum (565 nm pump and 601 nm probe) measured at each time delay: −14, −7 (both with probe laser pulses preceding the pump pulse), 0, 7, 14, 21, and 50 ps. Sample conditions and laser parameters are described in Figs. 1 and 2, respectively.

The population dynamics associated with the excited- and ground-states of the in vivo carotenoids can be observed in these PTR[3] spectra: (*a*) the −14 ps data are recorded outside the $\approx$8 ps cross-correlation period and therefore, no ground-state depletion or CSRS is observed.

(*b*) The −7 ps spectrum is recorded slightly within the pump/probe cross-correlation time and as a consequence, small negative features at 1,508 and 1,148 cm^{-1} resulting from the optically pumped depletion of the carotenoid ground state appear. In addition, two positive features appear: a narrow band at 1,063 cm^{-1} from the CSRS signal and a small, broad band near 1,767 cm^{-1} arising from the 2^1A_g population.

(*c*) The PTR[3] (0 ps) spectrum is recorded during the cross-correlation period and therefore, the influence of the pump laser is at a maximum. Ground-state depletion is near a maximum and consequently, the ground-state ^1A_g RR bands appear as large negative features (1,508, 1,148, 1,002, and 965 cm^{-1}). The RR bands assignable to the excited 2^1A_g state are at their largest positive values (i.e., 1,767 and 1,245 cm^{-1}) whereas the CSRS band at 1,063 cm^{-1} also reaches a maximum intensity. In addition, two new positive bands (1,468 and 1,119 cm^{-1}) appear on the low-frequency side of the strong, negative ground-state bands. These two features are attributed to RR scattering from vibrationally excited ground ^1A_g state populations. Similar results are found from the in vitro spirilloxanthin sample (*vide infra*). The initial population of the excited triplet ^3B_u state also may contribute to the RR scattering appearing at 1,468 and 1,119 cm^{-1}.

(*d*) The PTR[3] spectra at 7 and 14 ps delays contain more detailed information on the time evolution of all the ^1A_g, 2^1A_g, and ^3B_u populations. The intensity of the 1,063 cm^{-1} CSRS band decreases rapidly at 7 ps which lies just within the cross-correlation period and disappears completely at a 14 ps delay. The 1,767 and 1,245 cm^{-1} 2^1A_g bands also decrease rapidly over this same time period and are absent in the 14 ps spectrum (the small positive features near 1,265 and 1,343 cm^{-1} at 14 ps can be assigned to ^3B_u *vide infra*). The ^1A_g bands (negative), however, do not completely return to the zero intensity level at a 14 ps delay, but rather remain as relatively large negative features. This observation suggests that the original ^1A_g population has not been recovered by 14 ps. The formation of a vibrationally excited population which undergoes relatively slow vibrational relaxation within ^1A_g is consistent with such a conclusion. The intensities of several RR bands increase over the 7–14 ps interval (e.g., 1,484 and 1,124 cm^{-1})

appearing with relatively large positive values in the 14 ps spectrum.

(*e*) The PTR[3] spectrum recorded at 50 ps contains several new bands which correlate well with the previously reported RR spectrum of ^3B_u carotenoids in chromatophores of *Ch. vinosum* (9). The large negative bands assigned to ^1A_g have almost completely disappeared indicating that most of the original ground-state population has been recovered (i.e., vibrational relaxation is nearly complete). As previously reported (9), the ^3B_u population at 50 ps under these laser conditions represents only $\approx$2% of the total. The only transient population remaining after 50 ps is in ^3B_u which through PTR[3] spectra has been shown to decay in $\approx$2 ns (9). It should be pointed out that the relative intensities of the ^3B_u and 2^1A_g bands in Fig. 5 likely do not directly reflect the transient populations in the two excited electronic states. Both the resonance conditions with respect to the exciting laser wavelength and the vibrational modes giving rise to the corresponding bands (e.g., at 1,484 cm^{-1} for ^3B_u and at 1,767 cm^{-1} for 2^1A_g) may be considerably different.

The analogous difference RR spectra (PTR[3] minus probe only) from in vitro spirilloxanthin are presented in Fig. 6. These in vitro spectra are recorded at the same time delays as those used for the in vivo samples. The same ground-state depletion and transient 2^1A_g populations can be observed in the RR bands, but there is no indication that the ^3B_u state has been formed in the in vitro spirilloxanthin. As a consequence, these spectra are simpler than the corresponding in vivo spectra. Specifically, positive bands at 1,770, 1,468, 1,240, 1,202, and 1,125 cm^{-1} are assignable to excited-state species or populations whereas the negative bands at 1,505 and 1,148 cm^{-1} reflect ground-state depletion initiated by 565 nm excitation. There are no new bands appearing in the PTR[3] spectrum recorded at a 50 ps delay.

The time dependent intensities of the RR bands in these relatively simple spectra provide an opportunity to separate their respective assignments. The 1,770, 1,240, and 1,202 cm^{-1} bands have similar relative intensities at 0, 7, and 14 ps delays and are almost completely absent after 21 ps (decay rate $\approx$10 ps). This time dependence suggests an assignment to the 2^1A_g state. By contrast, the intensities of the negative RR bands at 1,505, and 1,148 cm^{-1} at 0 ps and 7 ps delays are about the same (perhaps slightly larger at 7 ps) and can be clearly observed with a 21 ps delay. The recovery time for the ^1A_g RR bands and the decay time of the 2^1A_g RR bands in the in vitro PTR[3] spectrum (Fig. 6), therefore, are not exactly the same. The difference demonstrates that ground-state recovery the spirilloxanthin involves more than one type of vibrational population and consequently, the time dependencies of the negative RR bands at 1,505 and 1,148

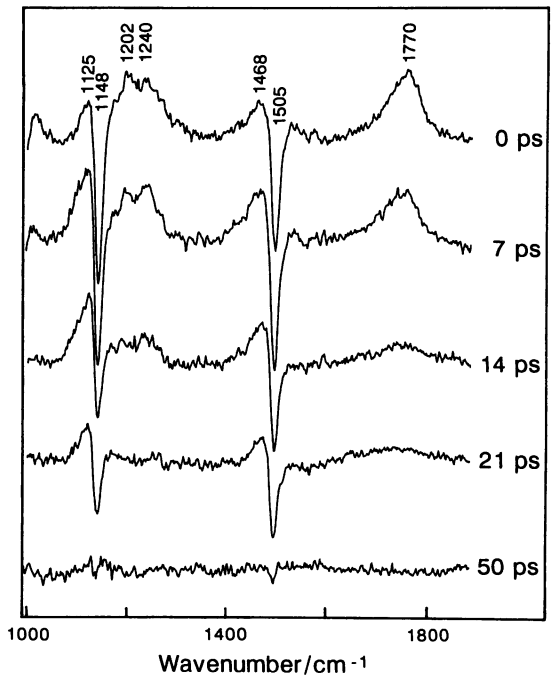

FIGURE 6 Population dynamics of excited and ground states of spirilloxanthin in benzene solution as viewed in PTR[3] spectra. The data are presented as difference spectra obtained by subtraction of the probe only spectrum measured at 601 nm from the PTR[3] spectrum (565 nm pump and 601 nm probe) measured at each time delay. Sample conditions and laser parameters are described in Figs. 1 and 2, respectively.

cm^{-1} reflect the contributions of each. Vibrationally excited ^1A_g levels, formed directly by the decay of the 2^1A_g state, again need to be considered. The difference in transient populations can be attributed to ^1A_g vibrational relaxation required to repopulate the original, thermalized vibrational levels present before 565 nm excitation. Such vibrational relaxation is completed within 50 ps.

This interpretation is supported by the appearance of asymmetrically broadened ^1A_g RR bands at short time delays. In the difference PTR[3] spectra presented in Fig. 6, such broadening is manifested as positive bands (1,468 and 1,125 cm^{-1}) appearing on the low-frequency side of the negative ^1A_g RR bands (1,505 and 1,148 cm^{-1}, respectively). The shifts to lower frequency displacements arise from anharmonicities in the vibrationally excited ^1A_g levels. The time dependent decay of these positive RR bands is the same as the recovery time of the corresponding negative RR bands (Fig. 6) suggesting that the populations being monitored are kinetically correlated. The same type of broadening on the low-frequency side of ground-state RR bands has been observed from bacteriorhodopsin samples and assigned

by PTR[3] scattering (using both Stokes and anti-Stokes data) as originating from vibrationally excited, ground-state populations (36).

A more detailed consideration of this interpretation suggests that evidence pertaining to the origin of the positive bands at 1,468 and 1,125 cm^{-1} may be found in the anti-Stokes Raman scattering from the samples. In fact, such measurements have been successfully performed by the present authors and published elsewhere (37). These time-resolved anti-Stokes Raman results provide more quantitative information on population dynamics including the vibrational relaxation times in the ground electronic state (37). Furthermore, it should be noted that these positive RR bands do not arise from molecules in low-energy vibrational levels which are in contact with an environment at an elevated temperature created by a combination of photon absorption and fast energy transfer. Finally, data which contradict the proposed interpretation should be mentioned. In β-carotene, the C = C stretching frequency is found to *increase* with increasing temperature whereas the C–C stretching frequency remains essentially unchanged (38).

When the time-dependence of RR band intensities in the in vivo and in vitro carotenoid PTR[3] spectra are compared, several additional points become clear:

(*a*) the decay of the 2^1A_g band is slightly slower in benzene solution of spirilloxanthin than in the chromatophore. Specifically in the chromatophore, the 1,767 cm^{-1} band at 7 ps is almost the half of its value at 0 ps and completely disappears at 14 ps. In benzene solution, on the other hand, the 1,770 cm^{-1} band at 7 ps has an intensity close to that observed at 0 ps and even at 14 ps, a weak band is observed. This difference in relaxation time can be attributed to the presence of an additional relaxation channel in the chromatophore such as energy transfer to the Bchls. The energy transfer efficiency is ≈30% in chromatophores of *Ch. vinosum* (27).

(*b*) The carotenoid 2^1A_g bands near 1,770 cm^{-1} are observed at almost the same position in both chromatophores and benzene solution (1,767 and 1,770 cm^{-1}, respectively). This is in contrast to the observation that the 2^1A_g band of carotenoids in *Rb. sphaeroides* is 51 cm^{-1} lower than that of the in vitro spheroidene (the major in vivo carotenoid) in *n*-hexane solution (21).

The considerably higher frequency of the C = C stretching mode in 2^1A_g (> 1,700 cm^{-1}) relative to that in ^1A_g (≈ 1,500 cm^{-1}) has been attributed to strong vibronic coupling between the 2^1A_g and ^1A_g states via this vibrational mode (17–24). It also has been shown, however, that the 2^1A_g C = C stretching frequency exhibits a significant solvent dependence which can be ascribed to vibronic coupling between the 2^1A_g and ^1B_u states (23). This solvent effect is observed through the decrease in the 2^1A_g C = C stretching frequency as the $^1B_u \leftarrow {}^1A_g$ absorption maximum shifts to the red. Although this solvent effect is larger in asymmetric carotenoids, even symmetric (ground-state) carotenoids such as β-carotene exhibit changes in the C = C stretching frequency as the solvent is changed (e.g., 1,793 cm^{-1} in pentane with λ_{max} = 447 nm versus 1,773 cm^{-1} in chloroform with λ_{max} = 462 nm) (23).

For the case of spirilloxanthin in the chromatophores of *Ch. vinosum* and in benzene solution, the absorption maxima are about the same and therefore, the C = C stretching frequencies can be compared directly. The similarity of the 2^1A_g C = C frequencies in these two environments suggests that no significant changes in the vibronic coupling occurs when spirilloxanthin is bound to the apoprotein. This conclusion is consistent with the observation that the ^1A_g C = C stretching frequencies also are about the same for in vivo and in vitro samples (1,508 and 1,505 cm^{-1}, respectively). If the vibronic coupling between the ^1A_g and 2^1A_g states is altered, the C = C frequencies in both states should change by the same magnitude, but in opposite directions. Recently, a low 2^1A_g C = C frequency for in vivo spheroidene (1,766 cm^{-1}) relative to its value in *n*-hexane solution (1,817 cm^{-1}) was explained in terms of a substantially weakened vibronic coupling between the ^1A_g and 2^1A_g states (21). Because the absorption maximum of spheroidene shifts by ≈25 nm between the in vivo and the *n*-hexane samples (27), however, it also is possible to interpret the low C = C stretching frequency in terms of a large environmental (i.e., solvent) change. In addition, a substantial change in the vibronic coupling contradicts the observation that the C = C stretching frequency in ^1A_g spheriodene is almost the same for the in vivo and *n*-hexane cases (< 6 cm^{-1} different [21]).

(*c*) The in vivo and in vitro PTR[3] spectrum can be clearly distinguished at a delay of 50 ps (Figs. 5 and 6). The RR spectrum of the excited ^3B_u state is evident in the in vivo spectrum whereas that from the in vitro spirilloxanthin in benzene solution contains essentially no RR structure. In benzene solution, spirilloxanthin completely relaxes to its ground ^1A_g state, including a vibrationally excited-state population (*vide infra*), whereas in the chromatophore, part of the 2^1A_g excited-state population relaxes to the ^3B_u state. Based on its risetime, this triplet state formation can be largely attributed to the fission process (3, 9, 28–32). This process requires the close proximity of carotenoid molecules either to other carotenoids or Bchls and therefore, relies on the spatial organization of the chromatophore. Such fission is unlikely to occur in dilute solution of carotenoids.

(*d*) The strong CSRS band at 1,063 cm^{-1} observed in chromatophore is not seen in the spirilloxanthin spectrum although the same pump and probe laser wavelength combination is used. Although requiring more

detailed study, this phenomenon may be associated with the spatial organization of the chromatophoric vesicles ($\approx$50 nm diameter) which provides the phase matching conditions required for efficient coherent Raman scattering that are absent in benzene solutions of spirilloxanthin. Alternatively, the third-order susceptibility of the carotenoid may be enhanced by specific interactions in the chromatophore itself.

After the submission of this present work, a paper dealing with the apparent breakdown of the phase matching condition in coherent anti-Stokes Raman scattering (CARS) was published (39). That observation was interpreted in terms of optical inhomogeneity of the liquid sample (39).

The authors wish to thank J. Fitch and T. Meyer in Professor Cusanovich's laboratory at the University of Arizona for their assistance in the preparation of in vivo samples. G. H. Atkinson gratefully acknowledges the Alexander von Humboldt-Stiftung and the Fulbright Grant Program for their support and Professor E. Schlag for his hospitality at the Technical University of Munich where part of this manuscript was prepared.

Partial support for this research was provided by a grant from the DuPont Company for the exchange of Japanese and American researchers and a grant (63045007) from the Ministry of Education, Science, and Culture of Japan.

Received for publication 13 December 1990 and in final form 28 March 1991.

REFERENCES

1. Siefermann-Harms, D. 1985. Carotenoids in photosynthesis. I. Location in photosynthetic membranes and light-harvesting function. *Biochim. Biophys. Acta.* 811:325–355.
2. Cogdell, R. J., and H. A. Frank. 1987. How carotenoids function in photosynthetic bacteria. *Biochim. Biophys. Acta.* 895:63–79.
3. Nuijs, A. M., R. van Grondelle, H. L. P. Joppe, A. C. van Bochove, and L. N. M. Duysens. 1985. Singlet and triplet excited carotenoid and antenna bacteriochlorophyll of the photosynthetic purple bacterium *Rhodospirillum rubrum* as studied by picosecond absorbance difference spectroscopy. *Biochim. Biophys. Acta.* 810:94–105.
4. Wasielewski, M. R., and L. D. Kispert. 1986. Direct measurement of the lowest excited singlet state lifetime of all-*trans*-β-carotene and related carotenoids. *Chem. Phys. Lett.* 128:238–243.
5. Wasielewski, M. R., D. M. Tiede, and H. A. Frank. 1986. Ultrafast electron and energy transfer in reaction center and antenna proteins from photosynthetic bacteria. *In* Ultrafast Phenomena V. G. R. Fleming and A. E. Siegman, editors. Springer-Verlag, Berlin. 388–392.
6. Gillbro, T., R. J. Cogdell, and V. Sundström. 1988. Energy transfer from carotenoid to bacteriochlorophyll *a* in the B800-820 antenna complexes from *Rhodopseudomonas acidophila* strain 7050. *FEBS (Fed. Eur. Biochem. Soc.) Lett.* 235:169–172.
7. Wasielewski, M. R., D. G. Johnson, E. G. Bradford, and L. D. Kispert. 1987. Temperature dependence of the lowest excited singlet-state lifetime of all-*trans*-β-carotene and fully-deuterated all-*trans*-β-carotene. *J. Chem. Phys.* 91:6691–6697.
8. Bondarev, S. L., S. M. Bachilo, S. S. Dvornikov, and S. A. Tikhomirov. 1989. $S_2 \rightarrow S_0$ fluorescence and transient $S_n \leftarrow S_1$ absorption of all-*trans*-β-carotene in solid and liquid solutions. *J. Photochem. Photobiol. B Biol.* A46:315–322.
9. Hayashi, H., S. Kolaczkowski, T. Noguchi, D. Blanchard, and G. H. Atkinson. 1990. Picosecond time-resolved resonance Raman scattering and absorbance changes of carotenoids in light-harvesting systems of photosynthetic bacterium *Chromatium vinosum*. *J. Am. Chem. Soc.* 112:4664–4670.
10. Trautman, J. K., A. P. Shreve, C. A. Violette, H. A. Frank, T. G. Owens, and A. C. Albrecht. 1990. Femtosecond dynamics of energy transfer in B800–850 light-harvesting complexes of *Rhodobacter sphaeroides*. *Proc. Natl. Acad. Sci. USA.* 87:215–219.
11. Trautman, J. K., A. P. Sheve, T. G. Owens, and A. C. Albrecht. 1990. Femtosecond dynamics of carotenoids to chlorophyll energy transfer in thylakoid membrane preparations from *Phaeodactylum tricornutum* and *Nannochlorpsis* sp. *Chem. Phys. Lett.* 166:369–374.
12. Sheve, A. P., J. K. Trautman, T. G. Owens, and A. C. Albrecht. 1990. Two-photon excitation spectroscopy of thylakoid membrane from *Phaeodactylum tricornutum:* evidence for an in vivo two-photon-allowed carotenoid state. *Chem. Phys. Lett.* 170:51–56.
13. Thrash, R. J., H. L. B. Fang, and G. E. Leroi. 1977. The Raman excitation profile spectrum of β-carotene in the preresonance region: evidence for a low-lying singlet state. *J. Chem. Phys.* 67:5930–5933.
14. Dallinger, R. F., S. Farquaharson, W. H. Woodruff, and M. A. J. Rodgers. 1981. Vibrational spectroscopy of the electronically excited state. 4. Nanosecond and picosecond time-resolved resonance Raman spectroscopy of carotenoid excited states. *J. Am. Chem. Soc.* 103:7433–7440.
15. Haley, L. V., and J. A. Koningstein. 1983. Space- and time-resolved resonance-enhanced vibrational Raman spectroscopy from a femtosecond-lived excited state of β-carotene. *Chem. Phys.* 77:1–9.
16. Wylie, I. W., and J. A. Koningstein. 1984. Photoisomerization and time-resolved Raman studies of 15,15′-*cis*-β-carotene and 15,15′-*trans*-β-carotene. *J. Phys. Chem.* 88:2950–2953.
17. Hashimoto, H., and Y. Koyama. 1989. The C = C stretching Raman lines of β-carotene isomer in the S_1 state as detected by pump-probe resonance Raman spectroscopy. *Chem. Phys. Lett.* 154:321–325.
18. Noguchi, T., S. Kolaczkowski, C. Arbour, S. Aramaki, G. H. Atkinson, H. Hayashi, and M. Tasumi. 1989. Resonance Raman spectrum of the excited 2^1A_g state of β-carotene. *Photochem. Photobiol.* 50:603–609.
19. Hashimoto, H., and Y. Koyama. 1989. Raman spectra of all-*trans*-β-apo-8′-carotenal in the S_1 and T_1 states: a picosecond pump-and-probe technique using ML-QS pulse trains. *Chem. Phys. Lett.* 162:523–527.
20. Hashimoto, H., and Y. Koyama. 1989. Raman spectra of all-*trans*-β-carotene in the S_1 and T_1 states produced by direct photoexcitation. *Chem. Phys. Lett.* 163:251–256.
21. Kuki, M., H. Hashimoto, and Y. Koyama. 1990. The $2^1A_g^-$ state of a carotenoid bound to the chromatophore membrane of *Rhodobacter sphaeroides* 2.4.1. as revealed by transient resonance Raman spectroscopy. *Chem. Phys. Lett.* 165:417–422.
22. Hashimoto, H., and Y. Koyama. 1990. The $2^1A_g^-$ state of a

carotenoid bound to spinach chloroplast as revealed by picosecond transient Raman spectroscopy. *Biochim. Biophys. Acta.* 1017:181–186.

23. Noguchi, T., H. Hayashi, M. Tasmui, and G. H. Atkinson. 1991. Solvent effects on the a_g C = C stretching mode in the 2^1A_g excited state of β-carotene and two derivatives: picosecond time-resolved Raman spectroscopy. *J. Phys. Chem.* 95:3167–3172.
24. Noguchi, T., H. Hayashi, M. Tasumi, and G. H. Atkinson. 1990. Frequencies of the Franck-Condon active a_g C = C stretching mode in the 2^1A_g excited state of carotenoids. *Chem. Phys. Lett.* 175:163–169.
25. Thrash, R. J., H. L. B. Fang, and G. E. Leroi. 1979. On the role of forbidden low-lying excited states of light-harvesting carotenoids in energy transfer in photosynthesis. *Photochem. Photobiol.* 29:1049–1050.
26. Gillbro, T., and R. J. Cogdell. 1989. Carotenoid fluorescence. *Chem. Phys. Lett.* 158:312–316.
27. Noguchi, T., H. Hayashi, and M. Tasumi. 1990. Factors controlling the efficiency of energy transfer from carotenoids to bacteriochlorophyll in purple photosynthetic bacteria. *Biochim. Biophys. Acta.* 1017:280–290.
28. Bensasson, R., E. A. Dawe, D. A. Long, and E. J. Land. 1977. Single → triplet intersystem crossing quantum yields of photosynthetic and related polyenes. *J. Chem. Soc. Faraday Trans. I.* 73:1319–1325.
29. Rademaker, H., A. J. Hoff, R. van Grondelle, and L. N. M. Duysens. 1980. Carotenoid triplet yields in normal and deuterated *Rhodospirillium rubrum. Biochim. Biophys. Acta* 592:240–257.
30. Frank, H. A., W. J. McGann, J. Macknicki, and M. Felber. 1982. Magnetic field effects on the fluorescence of two reaction centerless mutants of *Rhodopseudomonas capsulata. Biochem. Biophys. Res. Commun.* 106:1310–1317.
31. Kingma, H., R. van Grondelle, and L. N. M. Duysens. 1985. Magnetic-field effects in photosynthetic bacteria. I. magnetic-field-induced bacteriochlorophyll emission changes in the reaction center and the antenna of *Rhodospirillum rubrum, Rhodopseudomonas sphaeroides,* and *Prosthecochloris aestuarii. Biochim. Biophys. Acta.* 808:363–382.
32. Kingma, H., R. van Grondelle, and L. N. M. Duysens. 1985. Magnetic-field effects in photosynthetic bacteria. II. Formation of triplet states in the reaction center and the antenna of *Rhodospirillum rubrum* and *Rhodopseudomonas sphaeroides.* Magnetic-field effects. *Biochim. Biophys. Acta.* 808:383–399.
33. Hayashi, H., and S. Morita. 1980. Near-infrared absorption spectra of light-harvesting bacteriochlorophyll protein complexes from *Chromatium vinosum. J. Biochem. (Tokyo).* 88:251–258.
34. Atkinson, G. H., D. Blanchard, H. Lemaire, T. L. Brack, and H. Hayashi. 1989. Picosecond time-resolved fluorescence spectroscopy of K-590 in the bacteriorhodopsin photocycle. *Biophys. J.* 55:263–274.
35. Atkinson, G. H., T. Brack, D. Blanchard, and G. Rumbles. 1989. Picosecond time-resolved resonance Raman spectroscopy of the initial *trans* to *cis* isomerization in the bacteriorhodopsin photocycle. *Chem. Phys.* 131:1–15.
36. Brack, T. L., and G. H. Atkinson. 1991. Vibrationally-excited retinal in the bacteriorhodopsin photocycle: picosecond time-resolved anti-Stokes resonance Raman scattering. *J. Phys. Chem.* 95:2351–2356.
37. Hayashi, H., M. Tasumi, and G. H. Atkinson. 1990. Vibrationally-excited states in carotenoids: Picosecond time-resolved anti-Stokes resonance Raman spectroscopy. *Chem. Phys. Lett.* 175: 163–169.
38. Saito, S., M. Tasumi, and C. H. Euguster. 1983. Resonance Raman spectra (5800–40 cm^{-1}) of all-*trans* and 15-*cis* isomers of β-carotene in the solid state and in solution. Measurements with various laser lines from ultraviolet to red. *J. Raman Spectrosc.* 14:299–309.
39. Ishibashi, T., and H. Hamaguchi. 1990. Partially coherent anti-Stokes Raman scattering (PCARS). *Chem. Phys. Lett.* 175:543–547.